Stem Cell Research 32 (2018) 126–134

Contents lists available at ScienceDirect

Stem Cell Research

journal homepage: www.elsevier.com/locate/scr

Rapid and efficient differentiation of functional motor neurons from human iPSC for neural injury modelling

Fabio Bianchi[a], Majid Malboubi[a], Yichen Li[c], Julian H. George[a], Antoine Jerusalem[b], Francis Szele[c], Mark S. Thompson[a], Hua Ye[a,*]

[a] Institute of Biomedical Engineering, Department of Engineering Science, University of Oxford, OX3 7DQ, UK
[b] Department of Engineering Science, University of Oxford, OX1 3PJ, UK
[c] Department Physiology, Anatomy and Genetics, University of Oxford, OX1 3QX, UK

ARTICLE INFO

Keywords:
Induced pluripotent stem cells (iPSC)
Motor neuron differentiation
Electrophysiology
Neural injury

ABSTRACT

Primary rodent neurons and immortalised cell lines have overwhelmingly been used for *in vitro* studies of traumatic injury to peripheral and central neurons, but have some limitations of physiological accuracy. Motor neurons (MN) derived from human induced pluripotent stem cells (iPSCs) enable the generation of cell models with features relevant to human physiology. To facilitate this, it is desirable that MN protocols both rapidly and efficiently differentiate human iPSCs into electrophysiologically active MNs. In this study, we present a simple, rapid protocol for differentiation of human iPSCs into functional spinal (lower) MNs, involving only adherent culture and use of small molecules for directed differentiation, with the ultimate aim of rapid production of electrophysiologically functional cells for short-term neural injury experiments. We show successful differentiation in two unrelated iPSC lines, by quantifying neural-specific marker expression, and by evaluating cell functionality at different maturation stages by calcium imaging and patch clamping. Differentiated neurons were shown to be electrophysiologically altered by uniaxial mechanical deformation. Spontaneous network activity decreased with applied stretch, indicating aberrant network connectivity. These results demonstrate the feasibility of this rapid, simple protocol for differentiating iPSC-derived MNs, suitable for *in vitro* neural injury studies focussing on electrophysiological alterations caused by mechanical deformation or trauma.

1. Introduction

Supraphysiological elongation of peripheral nerves causes conduction blocks, resulting in chronic or temporary debilitating loss of motor function (Robinson, 2000; Miller, 1987). For example, brachial plexus birth palsy, initiated by excessive brachial plexus stretching during birth, causes motor and sensory impairment in 0.4% of US births (Abid, 2016). Conduction blocks implicate multiple nerve components including myelin (Sun et al., 2012), axonal paranodes (Rickett et al., 2011) and blood vessels (Ogata and Naito, 1986), but impairment of electrical transmission with strain has also been shown in isolated unmyelinated neuronal axons (Galbraith et al., 1993). Current studies on stretch-related conduction blocks are limited to animal tissue models (Sun et al., 2012; Rickett et al., 2011), and the majority of *in vitro* studies on the effect of mechanical injury on neurons are limited to using rodent primary neurons (Bar-Kochba et al., 2016; Kang et al., 2015), rodent neural stem cells (Kurtoglu et al., 2017), or immortalised cell lines (Skotak et al., 2012). Animal models provide simple, inexpensive models for neural damage studies, but concerns exist about the translational value of results from animal models to human conditions (Xiong et al., 2013). For example, candidate drugs for neuroprotection have failed human clinical trials after positive results in animal models (Marklund et al., 2006). The use of human induced pluripotent stem cells (iPSCs) provides physiologically relevant insights into the mechanics of human neural injury and motor function loss, overcoming potential issues of interspecies variability.

The induction of pluripotency in adult human cells provides an alternative cell source, both for *in vitro* studies and for clinical applications (Takahashi et al., 2007), avoiding ethical and regulatory complications of embryonic stem cell (ESC) use. Concerns about reproducibility and efficiency of iPSC differentiation, coupled with high costs and lengthy timeframes, have however limited their use (Kobold et al., 2015; Kim et al., 2014). Pluripotency induction by forced expression of defined factors generates iPSCs from adult cells, which can

The research materials supporting this publication can be accessed by contacting the corresponding author.

* Corresponding author.
E-mail address: hua.ye@eng.ox.ac.uk (H. Ye).

https://doi.org/10.1016/j.scr.2018.09.006
Received 13 May 2018; Received in revised form 6 September 2018; Accepted 10 September 2018
Available online 26 September 2018

then be differentiated into adult cell lineages, including multiple neural fates such as dopaminergic (Zhang et al., 2014), GABAergic (Sun et al., 2016) and motor neurons (MNs) (Faravelli et al., 2014), by following developmental cues found *in vivo* (Tao and Zhang, 2016). iPSC-derived neurons have multiple uses, including disease modelling (Sances et al., 2016), *in vitro* neural injury modelling (Sherman et al., 2016) and transplantation trials (Kobold et al., 2015), for which differentiation protcol requirements vary. In modelling diseases such as amyotrophic lateral sclerosis (ALS), cells must acquire the diseased phenotype, and generally need to be kept in culture for extended periods of time (Sances et al., 2016; Dimos et al., 2008). In injury modelling, the emphasis is on large scale, rapid production of functional cells, which are only kept in culture until experiments are performed (Sherman et al., 2016).

Current human iPSC MN induction protocols vary in timescale and efficiency, with few protocols achieving both high efficiency and rapid MN generation. Faravelli et al. reviewed MN induction protocols from both human ESCs and iPSCs, showing high variability in efficiency and timescale of protocols, ranging from 30 days to more than six weeks (Faravelli et al., 2014). Measures of efficiency include specific marker expression, morphological analysis, electrophysiological analysis and animal transplantation, and depend on the intended use for iPSC-derived MNs (Faravelli et al., 2014). Sances et al. reviewed protocols used to derive MNs specifically for ALS modelling, reporting differentiation efficiencies from 20% to 95% and with timeframes ranging from 12 to 130 days, but without taking into account the quality of characterisation, the protocol difficulty, or the intended MN use (Sances et al., 2016).

In directed differentiation, iPSCs are induced to become neural progenitor cells (NPCs) through neuralisation, either by embryoid body (EB) formation, or by dual SMAD inhibition in monolayer cultures. EB formation, where suspension cells spontaneously arrange and grow in three-dimensional aggregates upon withdrawal of factors promoting pluripotency, is the most widely used neuralisation method (Shimojo et al., 2015; Maury et al., 2015; Salimi et al., 2014; Amoroso et al., 2013). However, EB formation requires lengthy protocols, the use of undefined culture conditions often including animal serum (Salimi et al., 2014), and is tedious to perform (Chambers et al., 2009; Surmacz et al., 2012). More recently, techniques for neural neuralisation in adherent monolayer cultures have been developed, using defined small molecules for dual-SMAD signalling inhibition: bone morphogenic protein (BMP) and TGF-β/nodal/activin inhibition has been shown to effectively convert human iPSCs to NPCs in adherent cultures (Chambers et al., 2009; Li et al., 2011).

Noggin, an endogenous polypeptide, was the first factor to be used for BMP inhibition (Chambers et al., 2009), but selective small molecule BMP inhibitors dorsomorphin and DMH1 have been shown to increase inibition efficiency (Neely et al., 2012; Zhou et al., 2010). Additionally, TGF-β/activin/nodal inhibition by small molecule SB431542 has widely been used in both EB and monolayer cultures to induce neuralisation (Shimojo et al., 2015; Chambers et al., 2009; Inman et al., 2002). Following the establishment of adherent monolayer neuralisation protocols, additional factors have been tested to enhance neuralisation. CHIR-99021, a Wnt activator by GSK-3 inhibition, has been shown to further increase neuralisation efficiency, and notch signalling inhibition by γ-secretase inhibitor compound-E has been found to accelerate neuralisation (Li et al., 2011; Du et al., 2015).

NPCs, expressing transcription factors Sox1 and Pax6, and intermediate filament nestin, are then induced to MNs. Following *in vivo* gradients of retinoic acid (RA), responsible for MN specification along the rostrocaudal axis (Muhr et al., 1999), and hedgehog (HH), controlling ventral specification (Faravelli et al., 2014), NPCs are directed to motor neuron progenitors (MNPs) (Faravelli et al., 2014). Addition of soluble RA, and HH signalling activation by addition of direct smoothened agonist small molecules purmorphamine and SAG (Maury et al., 2015; Amoroso et al., 2013; Du et al., 2015), or of soluble sonic HH (SHH) (Zeng et al., 2010), result in OLIG2-positive MNPs. MNPs are then matured by culturing with growth factors, resulting in electrophysiologically functional spinal MNs, expressing MN-specific markers HB9, ISL1 and ChAT as well as neuron-specific markers such as β-III tubulin and MAP2 (Faravelli et al., 2014; Amoroso et al., 2013; Patani et al., 2011; Hu et al., 2010).

Here, we report the development of a fast induction protocol, aimed at rapid production of electrophysiologically active MNs for use in peripheral nerve mechanical injury studies. The aim was to rapidly produce adherent MN populations with high proportions of electrophysiologically active cells showing a mechanosensitive response to injury. Our protocol relies only on serum-free, adherent cultures, providing a facile method for the production of functional neurons. iPSCs monolayers are induced to NPCs in serum free conditions, by dual SMAD inhibition using dorsomorphin and SB431542, coupled with GSK-3 inhibition by CHIR-99021 and γ-secretase inhibition by compound-E. Following neuralisation, soluble RA, SHH, SAG, and purmorphamine are used to specify spinal MN fate. We assess MN maturity by whole cell patch clamping and calcium imaging, evaluating electrophysiological activity of differentiated neurons, and we characterise the mechanosensitivity of MNs generated by this protocol by measuring network activity modulation when subjected to uniaxial deformation. The differentiation protocol was validated in two iPSC lines independently reprogrammed from human dermal fibroblasts from unrelated control patients.

2. Materials and methods

2.1. iPSC culture

All reagents were purchased from ThermoFisher and growth factors from Peprotech unless otherwise specified.

Two iPSC lines were used in this study. Cell culture at all stages was carried out on tissue culture plastic well plates and imaging dishes (IBIDI μ-dish), unless otherwise specified. Line SB-AD3–1 was generated by StemBANCC, Oxford. In brief, dermal fibroblasts were obtained from skin biopsy of healthy individuals following appropriate ethical consent. iPSC generation was performed using the CytoTune-iPS 2.0 Sendai Reprogramming Kit (Invitrogen). The cultures undergoing reprogramming were maintained at 37 °C and 5% CO_2 in human ESC medium on feeder layers for two to three weeks or until colonies with typical human ESC morphology appeared. Individual colonies were mechanically dissected and plated onto fresh feeder plates for up to eight passages before being adapted to feeder free conditions which involved plating on Matrigel-coated plates (MG, Corning) with mTeSR1 media (Stem Cell Technologies), which was also the medium used in further experiments.

The second iPSC line (010S-1) was induced from a skin biopsy of a 18 year old female healthy subject, at the Highfield Unit, Warneford Hospital, Oxford. Skin fibroblasts were cultured from skin biopsy taken from the inner upper arm of the subject, and subsequently reprogrammed to iPSCs with CytoTune-iPS 2.0 Sendai Reprogramming Kit. The transfected cells were plated on mouse embryonic fibroblasts feeders to allow initial appearance of iPSC clones (about first 18 d). Picked clones were expanded, in a feeder-free manner, on Matrigel with mTeSR1 medium supplemented with 1% P/S. Colony 010S-1 was expanded to passage 13 and cryopreserved as the master stock. One vial from the master stocks was thawed in mTeSR medium on matrigel coated plates to perform quality control steps (data not shown) including normal speed of growth after thawing, CytoTune clearance assay by qPCR, flow-cytometry analysis of pluripotency markers NANOG and TRA-1-60, and SNP analysis of genomic integrity using an Illumina Human CytoSNP-12v2.1 beadchip array.

MG was diluted on ice in cold KnockOut-DMEM according to the batch-specific dilution factor, and added to well plates for 4–12 h before cell seeding. Thawed cells were plated in mTeSR supplemented with 1%

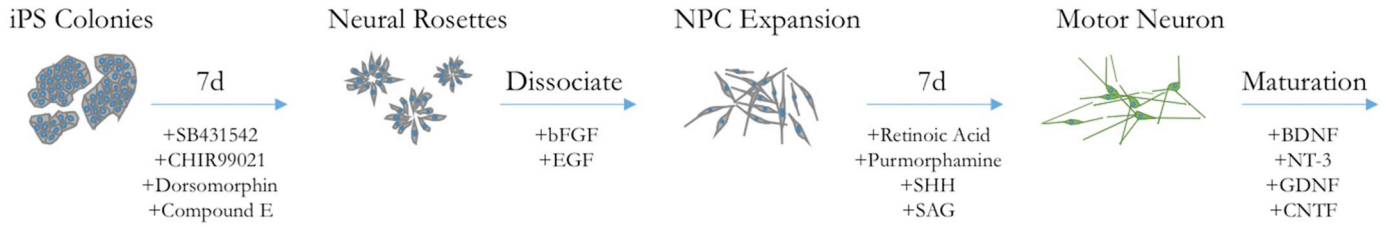

Fig. 1. Differentiation timeline. iPS colonies were neuralised by dual-SMAD, GSK-3 and γ-secratase inhibition for 7 days. Dissociated neural rosettes were expanded before differentiation to MN by caudalisation and ventralisation for 7 days.

Penicillin/Streptomycin and 1% RevitaCell (ROCK inhibitor and anti-oxidant compound) was added during the initial 24 h *medium* was replaced daily. Colonies were passaged by incubating for 3.5 min in versene (0.48 nM EDTA), lifted by washing with mTeSR medium using a large-bore pipette, and plated in mTeSR.

2.2. iPSC differentiation to NPC

The differentiation protocol (Fig. 1) was performed using iPS line SB-AD3–1, and validated in line 010S-1 by evaluating differentiation end-points (neuron staining and electrophysiology).

Confluent iPSCs were dissociated using accutase and plated at 0.5×10^6 cells/well on MG-coated 6-well plates in neural induction medium (NIM), consisting of a 1:1 mix of KO-DMEM/F:12 and neurobasal medium (NBM) supplemented with 10% KnockOut Serum Replacement, 1% Non-Essential Amino Acids (NEAA), 1% GlutaMAX, 0.1 mM L-ascorbic acid (L-AA, Sigma-Aldrich), 2 μM SB431542 (Cell Guidance Systems), 3 μM CHIR99021 (Sigma Aldrich), 1 μM dorsomorphin (StemCell) and 1 μM compound E (StemCell). 1% RevitaCell was added for the first 24 h only.

NIM was replaced daily for six days, after which cells were dissociated with Accutase, and plated in NPC expansion medium, consisting of a 1:1 mix of KO-DMEM:F12 and NBM, supplemented with 1% P/S, 1% B27, 1% N2, 1% NEAA, 1% GlutaMAX, 0.1 mM L-AA, 10 ng/mL bFGF and 10 ng/mL EGF. Cells were either expanded for banking, or kept for MN differentiation. One fifth of cells were retained at each passage for marker analysis. Cells were expanded for up to 4 passages.

2.3. NPC differentiation and MN maturation

NPCs were cultured for 6 days in MN induction medium, consisting of a 1:1 mix of KO-DMEM:F12 and Neurobasal Medium supplemented with 1% P/S, 1% B27, 1% N2, 1% Non-Essential Amino Acids, 1% GlutaMAX, 0.1 mM L-ascorbic acid, 10 μM all-trans retinoic acid (Sigma Aldrich), 100 ng/ml recombinant SHH, 1 μM Purmorphamine (Abcam) and 1 mM SAG Dihydrochloride (Sigma Aldrich). After seven days, cells were dissociated using Accutase, and re-plated in maturation medium, consisting of 1:1 KO-DMEM:F12 and NBM, supplemented with 1% P/S, 1% B27, 1% N2, 1% NEAA, 1% GlutaMAX, 0.1 mM L-AA, 10 ng/mL CNTF, 10 ng/ml BDNF, 10 ng/mL NT-3 and 10 ng/mL GDNF.

2.4. Immunocytochemistry, imaging and analysis

Cells were fixed in 3.75% paraformaldehyde (Sigma Aldrich) solution in phosphate buffered saline (PBS), blocked and permeabilised using 0.1% Triton-X, 0.1% Tween-20 and 2.5% BSA in PBS. Primary antibodies (all from AbCam, at 1:1000 unless specified) to Sox1, Pax6, Nestin, HB9, MAP2, NeuroFilament, Tuj1 and Olig2 (1:300, Millipore) were added, and counter-stained with AlexaFluor secondary antibodies. Nuclei were labelled with NucBlue. Cells were imaged using a Nikon TI-E inverted fluorescence microscope. Image analysis was carried out using ImageJ. Statistical analysis was carried out using GraphPad PRISM.

2.5. Calcium activity

Calcium activity was imaged using Oregon Green 488 BAPTA-2 calcium indicator (Grienberger and Konnerth, 2012). Cells were incubated in a 4 μM dye solution in FluoroBrite-DMEM Imaging Medium for 30 min, washed twice in PBS, and further incubated in fresh FB-DMEM for 30 min. Cells were imaged using standard FITC filters at 10 fps for 4 min, and fluorescence intensities from individual segmented cells recorded in time. Intensity values were adjusted for fluctuations by subtracting average background, and expressed as $I = \frac{I(t)}{I(t=0)}$.

2.6. Electrophysiology

A Digidata 1440A digitizer and a MultiClamp 700B amplifier piloted through pCLAMP 10 Software (all from Molecular Devices, CA) were used. Intracellular solution contained 140 mM KCl, 5 mM NaCl, 0.5 mM $CaCl^2$, 2 mM $MgCl^2$, 10 mM HEPES, 1 mM GTP, and 2 mM ATP, and was adjusted to 7.4 pH by KOH and 300 Osm L^{-1} by glucose addition. Bath solution contained 130 mM NaCl, 5 mM KCl, 2 mM $CaCl^2$, 1 mM $MgCl^2$, 10 mM glucose, and 10 mM HEPES (all from Sigma-Aldrich), and was adjusted to 7.4 pH by NaOH and 290 Osm L^{-1} by glucose addition. Following gigaseal formation, whole-cell patch clamp was established. Initially, a higher range of voltages (−70 to +70 mV) was used to elicit a response and to establish conditions under which gigaseal formation occurred reliably. Ion currents were then recorded within a lower range to avoid cell injury by stimulation from −50 to +30 mV under voltage-clamp recording, and action potentials (APs) were evoked in current clamp mode by stimulating current pulses from −50 pA to +30 pA.

2.7. Cell injury methods

Cell mechanosensitivity was tested by applying uniaxial strain to maturing cell networks. Previuosly, similar methods have been used to replicate *in vitro* traumatic brain injury, using rodent primary neurons (Magou et al., 2015; Pfister et al., 2003). A custom-built substrate deformation device, allowing simultaneous uniaxial cell deformation and high-frequency imaging was used to apply graded strains of up to 70% and 0.1 s^{-1} strain rate, with simultaneous network activity monitoring by calcium imaging. Cells were strained, and calcium flux was imaged for 4 min from cells kept in the strained state. MNs were seeded onto MG-coated custom-made rectangular deformable silicone wells with ultra-thin (50 μm) silicone culture surfaces measuring 10.0 mm × 6.5 mm at a density of 500 cells/mm^2 in maturation medium, and kept in culture two days before experiments.

2.8. Data analysis and statistics

Images were analysed using FIJI (Fiji Is Just ImageJ), and calcium imaging data was processed using a custom-written MATLAB code to filter data, extract and measure peaks. Statistical analysis was carried out using GraphPad PRISM v6.

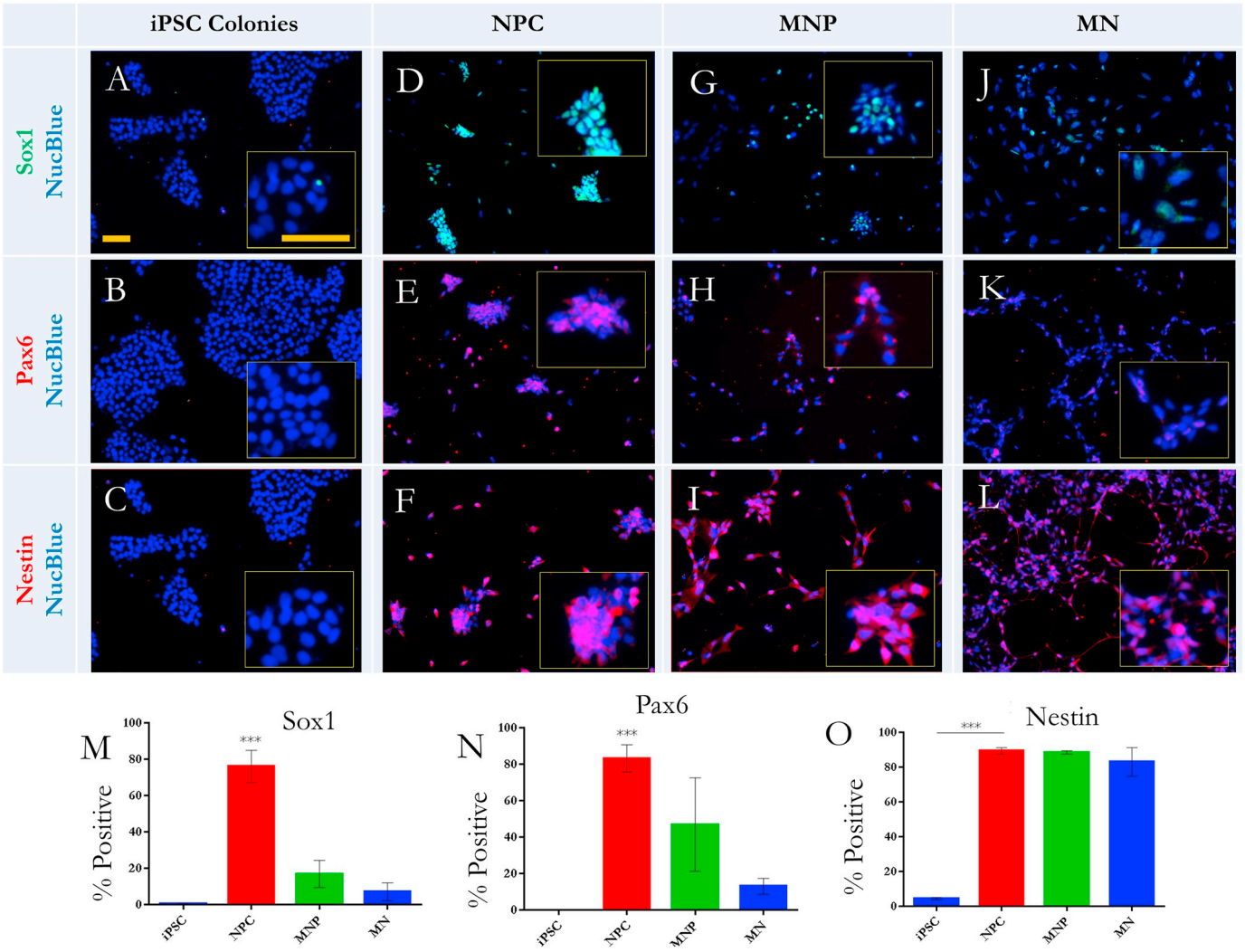

Fig. 2. Undifferentiated iPSC colonies did not express neural progenitor markers (A-C). iPSCs neuralised by dual SMAD, γ-secretase and GSK-3 inhibition formed neural rosettes and express neural Progenitor Markers Sox1, Pax6 and Nestin (D-F). Expression was reduced after MN specification (G-I) and maturation (J-L). Quantification of marker expression (M-O), bars show mean ± SD, n > 3, **** = $p < 0.0001$, *** = $p < 0.005$ by Anova testing with Tukey's multiple comparisons. Scale bars = 100 μm. Insets show high-magnification images of cells.

3. Results

3.1. iPSCs differentiate to MNs

During neuralisation, cell morphology changed from expanding colonies to neural rosettes, with radially arranged cell groups. Neuralisation was quantified after six days by expression of Sox1, Pax6 and Nestin. Increase of Pax6, Sox1 and Nestin positive cells were observed in neuralised samples, compared to undifferentiated iPSC colonies (Fig. 2). 76% ± 10% of neuralised cells expressed Sox1, 83% ± 11% expressed Pax6 and 89% ± 2% expressed nestin, all significant increases from iPSC.

MN specification induced a significant decrease in Pax6 and Sox1, whilst Nestin levels did not decrease significantly (Fig. 2). Olig2 expression after five days MN induction was significantly increased, with 88% ± 2% of cells positive for Olig2, indicating specification of MN fate. No significant Olig2 expression was detected in NPCs. Expression of Tuj1 also increased significantly, with 89% ± 4% of cells expressing β-III tubulin, showing induction to neural lineage (Fig. 3).

3.2. MN maturation

Cell morphology was altered during maturation, with reduced cell soma area and membrane spreading, and thin, extended projections connecting adjacent cells (Fig. 4 G). After 21 days in maturation medium, NPC marker expression was reduced significantly (Fig. 2), and neuron-specific structural proteins, Tuj1 (β-III Tubulin), NeuroFilament and MAP2, were expressed (Fig. 4). Synaptophysin was detected at cell junctions, suggesting synaptic connectivity. Positive staining for ChAT in somatas and HB9 in nuclei confirmed MN lineage for maturing cells (Fig. 4), with 73 ± 5% of cells positive for MN-specific HB9.

3.3. Efficiency of maturation to functional MNs

Neurons cultured in maturation medium for five days showed some calcium activity, with low spike magnitude and rate, and no bursting activity. Ion currents and induced APs were weak, indicative of successful differentiation but insufficient maturation (Fig. 5, A, B, D and E). Neurons cultured in maturation medium for 21 days showed faster rising spikes, higher spiking frequency, some bursting behaviour, defined ion currents, and induced APs, all indicative of neurons successfully maturing towards active cells (Fig. 5). After 21 days maturation,

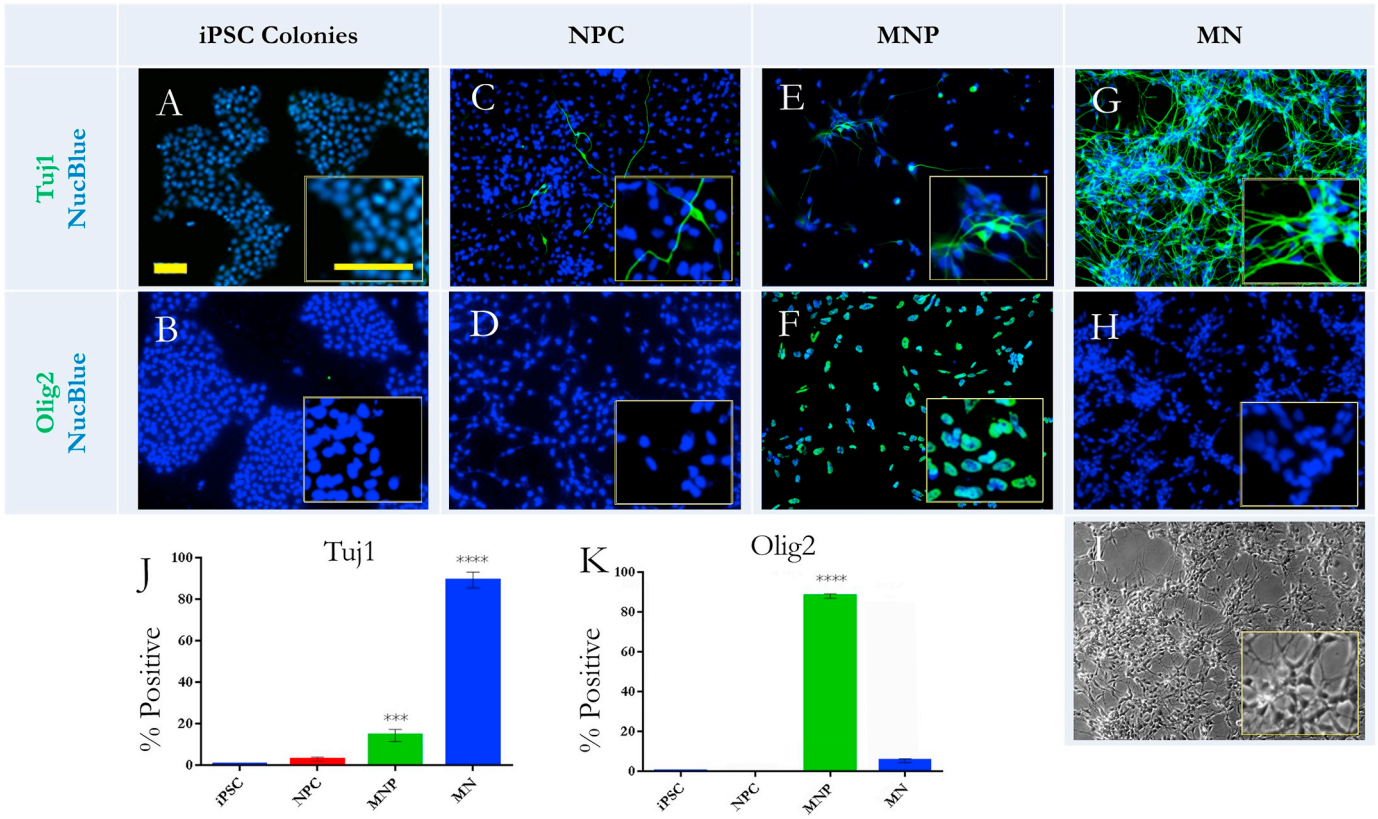

Fig. 3. Undifferentiated iPSC colonies did not express Tuj1 and Olig2 (A,B). NPCs showed low Tuj1 expression, and absence of Olig2 (C,D). MN specification increased Tuj1 expression (E), and induced significant Olig2 expression (F). MNs expressed Tuj1 (G) but no Olig2 (H). MNs show neuronal morphology with small somatas and extensive neurite networks (I). Quantification of marker expression (J,K), bars show mean ± SD, n > 3, *** = p < 0.005 by one way unpaired Anova testing with Tukey's multiple comparisons. Scale bars = 100 µm. Insets show high-magnification images of cells.

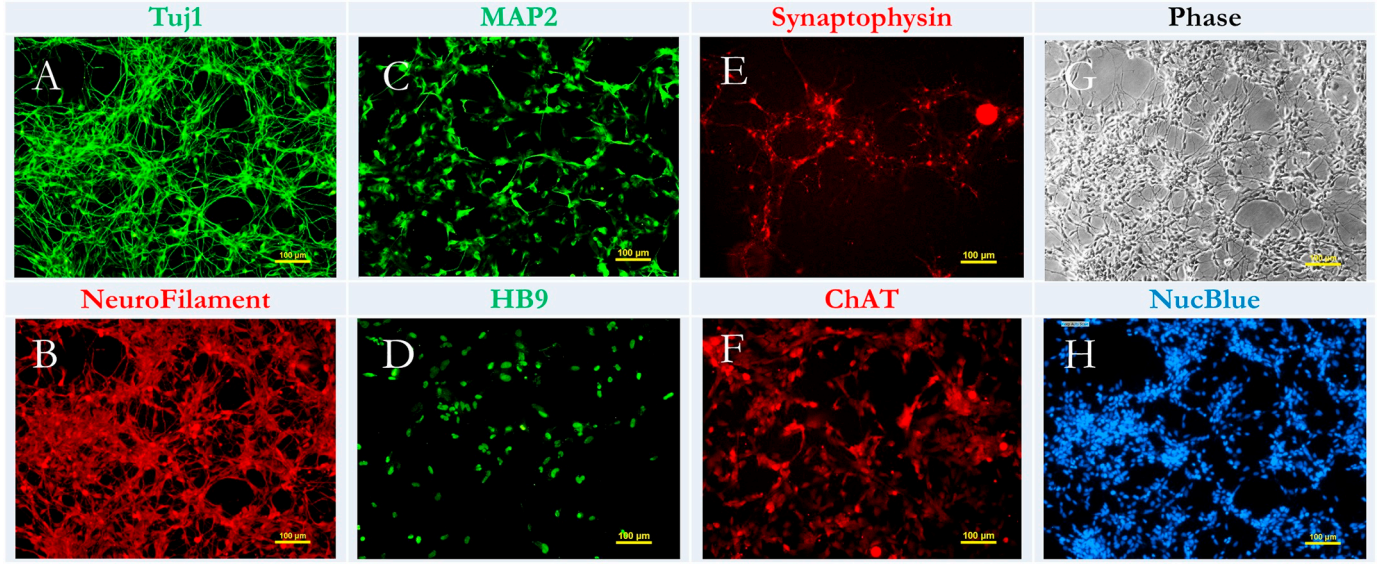

Fig. 4. Differentiated MNs expressed neural structural proteins Tuj1 (A), NF (B), MAP2 (C), MN specific markers HB9 and ChAT (D,F) and Synaptophysin (E). Phase contrast imaging showed elongated morphology (G). Cells were counterstained by NucBlue (H).

75% ± 3% of cells ($N = 8$ independent culture dishes) were active, significantly more than after day 5 of maturation (Fig. 5, C). The average magnitude of calcium spikes, measured as a percentage of the baseline value, was 4.8% at day 5, and 15.2% at day 21 of maturation. The ratio of rise to fall time of peaks was 0.42 and 0.29 and the average rise slope was 0.035 and 0.095, at day 5 and day 21 respectively.

3.4. iPSC-derived MNs form functional connections

Network connectivity at maturation day 21 was assessed from calcium imaging recordings. Spontaneous oscillations in intracellular calcium have been widely used as an indirect reporter of neural activity, as well as of functional synaptic connectivity (Grienberger and Konnerth, 2012; Wang and Gruenstein, 1997). Detection of concurrent calcium

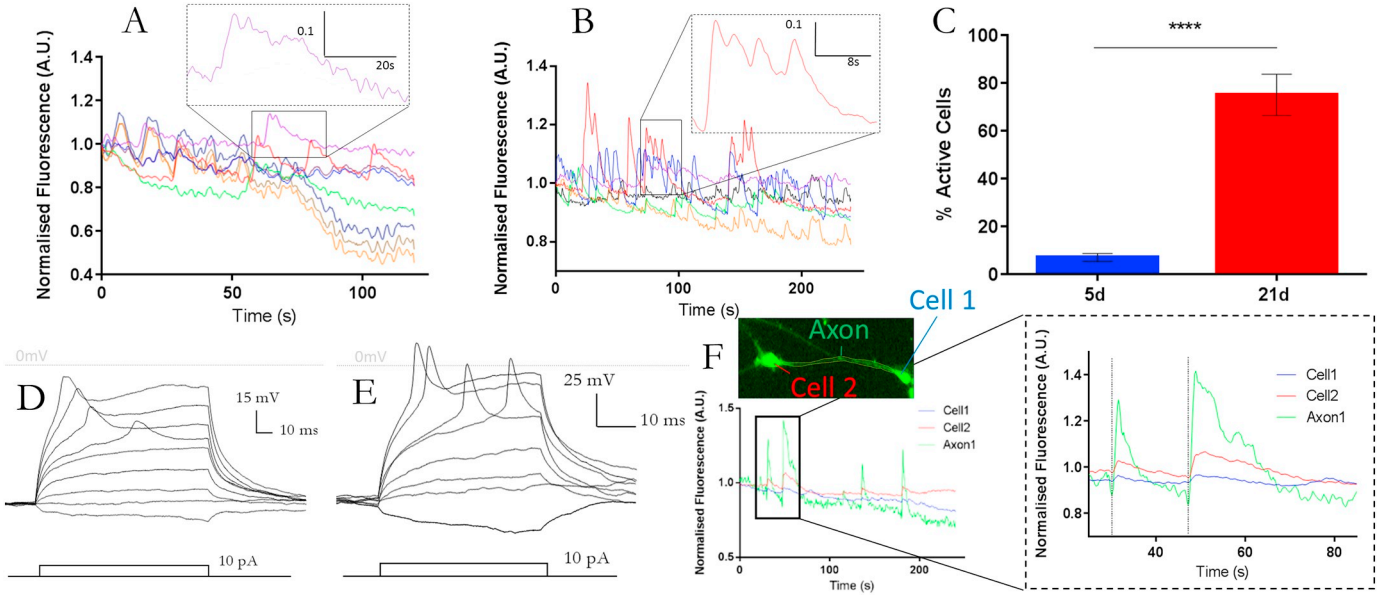

Fig. 5. Immature MNs showed low magnitude, low frequency calcium activity. Insert shows characteristic peak shape (A). Cells cultured in maturation media for 21 days showed higher frequency firing, with some bursting behaviour. Inset shows characteristic peak shape (B). Maturation for 21 days induced 75% of cells to active neurons, compared to 7% at day 5 (C, $n = 8$, **** = $p < 0.0001$ by unpaired *t*-test). Patch clamping current-clamp recordings showed immature neurons at day 5 (D) and maturing neurons at day 21 (E). Neurons formed connected networks, with signals propagating down axons between cells (F).

spikes in distinct neuron somatas was used as a marker of connectivity, as previously used in whole-brain network reconstruction (Mann et al., 2017). Maturing neurons successfully formed synaptic connections. Connected cells showed synchronised action potential firing, traceable along the connecting axon (Fig. 5). Cell connectivity was observed in all samples of maturing MNs tested (N = 8), indicating that neurons formed functional networks. No connectivity was observed after 5 days of maturation, indicating network maturation in time. To further confirm this, positive synaptophysin puncta staining was observed in neural cultures after 21 days in maturation medium (Fig. 4).

3.5. Validation of differentiation to maturing MN

Successful differentiation was validated by repeating the protocol using iPSC line 010S-1, and evaluating end-point functionality and neural marker expression as 010S-1 cells differentiate to motor neurons. After 21 days in maturation medium, cells show extensive neurite networks, and electrophysiological activity indicative of maturation. Voltage-clamp experiments show induced action potentials (Fig. 6 (A)), including AP train firing (Fig. 6 (B)). Calcium imaging analysis shows functional network connectivity, as previously shown in cell line SB-AD3–1 (Fig. 6 (C)). Marker staining shows positive expression of NPC markers after seven days neuralisation (Fig. 6 (D-G)), and positive expression of MN markers after 21 days maturation (Fig. 6 (H—K)). Qualitatively, cells tend to become more confluent during the same culture time, and a higher percentage of cells starts expressing Tuj1 early, compared to the same timepoint staining of NPC derived from SB-AD3–1 (Fig. 6 (E) *vs*Fig. 3 (C)).

3.6. Deformation injury affects network activity

Uniaxial stretch of cultured neurons has been previously used as a model for traumatic brain inury (TBI), where primary embryonic rat hippocampal neurons have been shown to respond to stretch by a marked decrease in spontaneous activity (Magou et al., 2015). However, inter-species differences in response to stretch injury possibly decrease the translational value of these results, and provide motivation to develop human iPSC-based *in vitro* models (Sherman et al., 2016). In order to test the response of iPSC-derived MN spontaneous calcium oscillations to uniaxial stretch, MNs matured for 21 days were subjected to increasing levels of stretch (25%, 45% and 75% strain at 0.1 S^{-1} strain rate), during which calcium imaging recordings were performed. Network activity was measured by calcium imaging for 4 min before deformation, and at each sequential deformation level. The number of active cells, measured as the percentage of cells within the field of view exhibiting spontaneous calcium spikes, decreases linearly with applied deformation, and does not recover immediately after stretch release (Fig. 7). A significant decrease in active cells was observed at each level, both compared to the un-stretched (control) condition, and compared to the previous stretch level (incremental effect).

4. Discussion

The establishment of simple, reproducible protocols for successful differentiation of human iPSC is paramount for facilitating more widespread use of iPS-derived cells for human *in vitro* MN injury modelling. Here, we aimed to develop a simple, rapid protocol for the efficient directed differentiation of electrophysiologically active, MNs from human iPSCs, aimed at producing active cultures for short-term neural injury studies. Efficiency of differentiation was measured by specific marker expression, and number of electrophysiologically active cells, measured in synaptically active networks, indicating cell populations suitable for neural injury experiments. The mechanosensitivity of cells was evaluated by exposing spontaneously active networks to uniaxial strain, and recording changes in network activity.

Adherent culture differentiation by dual-SMAD inhibition eliminates the need for EB formation, a complex and inefficient culture technique widely used in iPSC neural differentiation protocols (Shimojo et al., 2015; Maury et al., 2015; Salimi et al., 2014; Zhou et al., 2010), and increases efficiency of neuralisation (Faravelli et al., 2014; Sances et al., 2016; Chambers et al., 2009). Here, we combine dual-SMAD inhibition with wnt activation and γ-secretase inhibition, to further increase efficiency, resulting in 83% PAX-6 and 76% Sox1 positive NPCs after 6 days. Previous use of four neuralisation factors involved either EB formation or suspension culture step following neuralisation, and did not demonstrate efficiency in terms of electrophysiological maturation of cells and networks (Shimojo et al., 2015; Du et al., 2015). NPCs are induced to MNPs by dual HH activation, through addition of

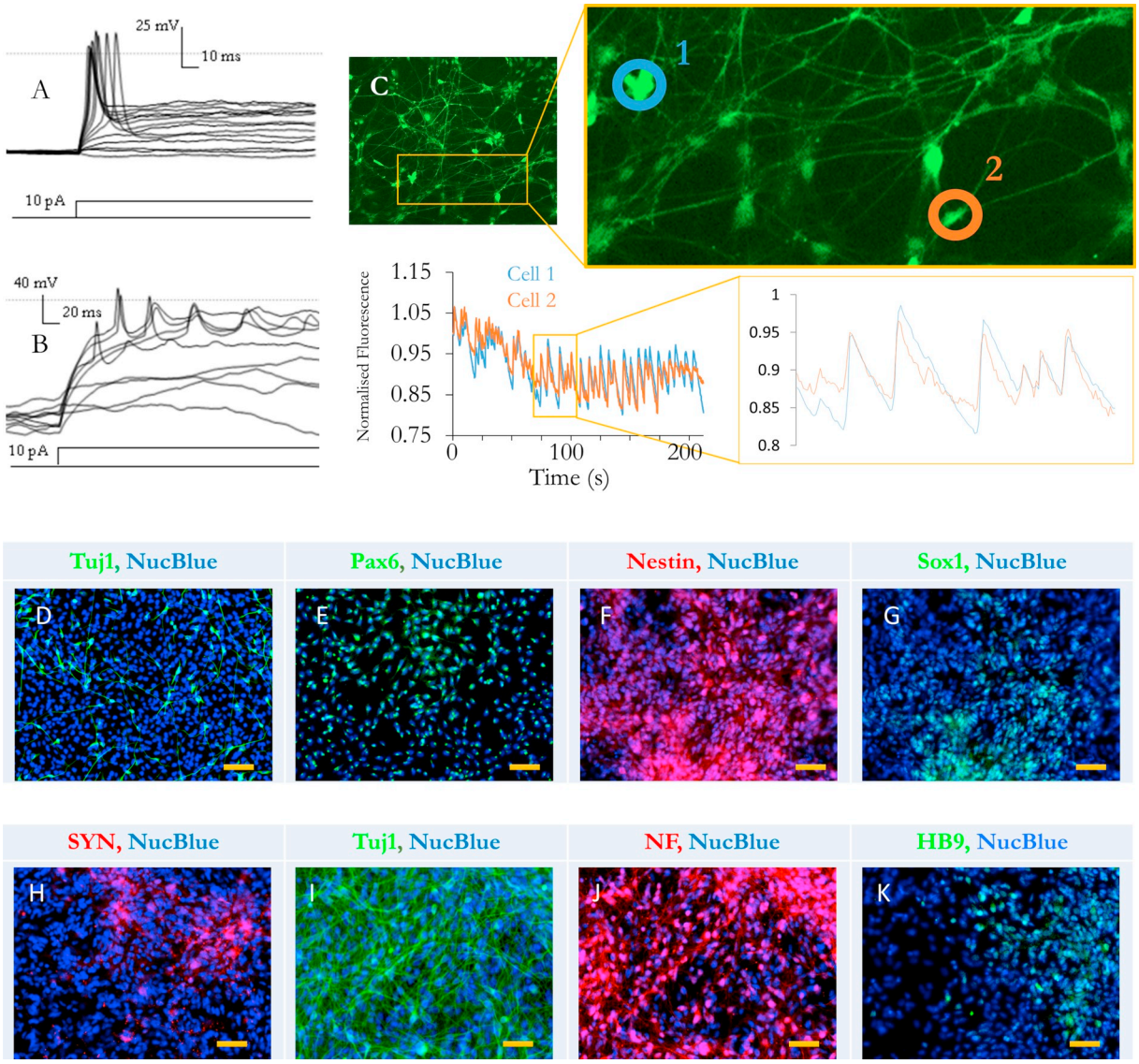

Fig. 6. Neural differentiation and maturity is validated by differentiation of independently induced iPS line 010S-1. After 21 days maturation, cells show strong induced AP signals (A), including AP train bursts (B), networked spontaneous activity (C). Staining of NPCs shows positive expression of NPC markers (D-G) and staining of maturing neurons shows positive expression of MN markers (H—K). Scale bar = 100 μm.

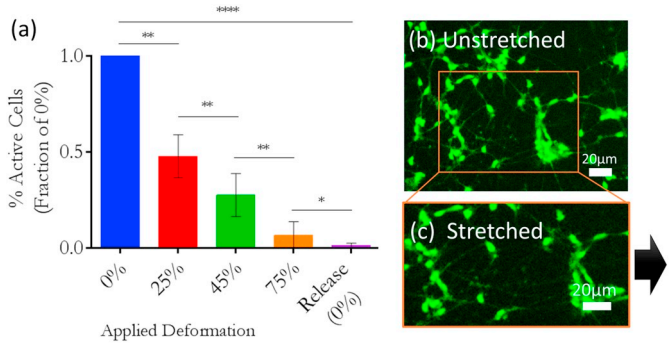

Fig. 7. Deformation of active networks (a) modulates spontaneous activity. With increased applied substrate deformation, the percentage of active cells decreases. $n = 7$ independent samples. **** = $p < 0.0001$, ** = $p < 0.01$, * = $p < 0.05$, by one way paired ANOVA with Tukey's multiple comparisons. Cell bodies and neurites (b) are subjected to deformation (c). Arrow indicates direction of stretch. Scale bars = 20 μm.

soluble SHH and direct smoothened activators purmorphamine and SAG. This results in highly pure MNP populations, with 88% of cells positively expressing OLIG2, in line with the highest values reported in literature (Hu and Zhang, 2010; Karumbayaram et al., 2009).

After 21 days in maturation medium, 89% of cells positively expressed Tuj1, 73% of cells positively expressed MN-specific HB9, and 75% of cells differentiated to electrophysiologically functional MNs within five weeks from iPSC thawing. Other protocols validated by electrophysiology range between 20 and 70% efficiency, and between 5 and 18 weeks duration (Faravelli et al., 2014; Sances et al., 2016). After 21 days of maturation, we show functional network formation by calcium imaging, positive expression of punctuated synaptophysin suggesting synapse formation, and positive expression of motor-neuron specific factors HB9 and cHAT, combined with neural-specific markers Tuj1, MAP2 and NeuroFilament. Moreover single-cell electrophysiology shows how, after 21 days, induced APs can be recorded, and waveform analysis of calcium spikes indicates maturation, with an increase in spike magnitude, decrease in rise and fall time, and increase in rise rate (Biffi et al., 2013). The same protocol was validated in 010S-1 cell line, a human dermal fibroblast derived iPSC line, unrelated to the SB-AD3–1

line, showing electrophysiological characteristics after 21 days maturation, and expression of neural progenitor and neural markers, confirming successful differentiation. For both cell lines, videos of calcium activity can be seen in supplementary material V1 and V2.

Maturing MNs forming spontaneously active networks were stretched to evaluate cell mechanosensitivity. Uniaxial strain can be used to model the mechanical environment of the peripheral nerve under physiological and traumatic conditions, where movement induces elongation along the nerve axis deforming tissues and neural fibres, and can be used to model peripheral nerve traumas such as increased strains due to carpal tunnel syndrome, joint dislocation, or iatrogenic aberrant limb positioning (Bueno and Shah, 2008; Topp and Boyd, 2006). A significant decrease in cells exhibiting spontaneous calcium spiking was observed during deformation, and no recovery of activity was measured following stretch release. This is consistent with results reported for primary embryonic and neonatal cortical and hippocampal rat neurons subjected to stretch (Magou et al., 2015; Prado et al., 2005; Goforth et al., 2011), and confirms that human iPSC-derived MNs are suitable for use in neural injury experiments. Videos of calcium activity in networks before and after stretch can be seen in supplementary materials V3 and V4. We present the first human MN-specific *in vitro* injury model, focussing on electrophysiological alterations caused by mechanical deformations, to provide a human relevant cell model for the study of mechanical deformation and injury.

Using MN-only cultures allows the functional response of neurons to stretch to be isolated. To further develop this as an *in vitro* model of human PNI, co-culture with Schwann cells could provide myelination, a key component of the nervous system which is disrupted by mechanical trauma (Sun et al., 2012), and that enhances neuron maturation and long-term survival. To maintain the premise of physiological relevance to human PNI, human stem cell-derived Schwann cells should be used. Although human iPSC-derived neurons have been myelinated by rodent primary Schwann cells (Clark et al., 2017), and human fibroblasts have been successfully reprogrammed to myelinating Schwann cells (Mazzara et al., 2017), to the best of our knowledge no co-culture model exists that would allow the development of a stem-cell derived human myelinated PNI injury model.

5. Conclusions

In summary, we present a protocol to facilitate the production of electrophysiologically active MNs from human iPSCs, for short-term cultures, aimed at *in vitro* human neural injury modelling. In 5 weeks from iPSC culture establishment, we show efficient differentiation of electrophysiologically active neurons, with 75% of cells showing spontaneous calcium activity, and expressing neural and MN markers. Compared to other protocols showing electrophysiological maturity, this represents an improvement in terms of time as well as in efficiency. We show that human iPSC-derived MNs are suitable for *in vitro* neural injury modelling by measuring functionality alterations in networks exposed to uniaxial strain. This protocol improves efficiency of rapid MN directed differentiation, producing populations of highly active neurons expressing MN specific markers within 5 weeks, providing an accessible, easily implementable alternative to animal cells. Despite maintaining advantages in terms of cost, complexity and range of applications, concerns raised over the translational value of rodent models in neurotrauma, including differences in nociception (Rostock et al., 2017) and response to traumatic injury (Povlishock et al., 1994), indicate the importance of developing *in vitro* alternatives using human cells.

Supplementary data to this article can be found online at https://doi.org/10.1016/j.scr.2018.09.006.

Acknowledgements

The authors would like to acknowledge Dr. Zameel Cader and Dr. Satyan Chintawar for kindly providing SB-AD3–1 cells through StemBANCC. Authors acknowledge China Regenerative Medicine Limited (CRMI) for funding and the EPSRC DTP award number 1514540 for F.B. funding. M.B. and A.J. acknowledge funding from the European Union's Seventh Framework Programme (FP7 2007-2013) ERC Grant Agreement No. 306587.

References

Abid, A., Feb. 2016. Brachial plexus birth palsy: Management during the first year of life. Orthop. Traumatol. Surg. Res. 102 (1 Suppl), S125–S132.
Amoroso, M.W., et al., Jan. 2013. Accelerated high-yield generation of limb-innervating motor neurons from human stem cells. J. Neurosci. 33 (2), 574–586.
Bar-Kochba, E., Scimone, M.T., Estrada, J.B., Franck, C., Aug. 2016. Strain and rate-dependent neuronal injury in a 3D in vitro compression model of traumatic brain injury. Sci. Rep. 6, 30550.
Biffi, E., Regalia, G., Menegon, A., Ferrigno, G., Pedrocchi, A., Dec. 2013. The influence of neuronal density and maturation on network activity of hippocampal cell cultures: a methodological study. PLoS One 8 (12), e83899.
Bueno, F.R., Shah, S.B., Sep. 2008. Implications of tensile loading for the tissue engineering of nerves. Tissue Eng. Part B Rev. 14 (3), 219–233.
Chambers, S.M., Fasano, C.A., Papapetrou, E.P., Tomishima, M., Sadelain, M., Studer, L., Mar. 2009. Highly efficient neural conversion of human ES and iPS cells by dual inhibition of SMAD signaling. Nat. Biotechnol. 27 (3), 275–280.
Clark, A.J., Kaller, M.S., Galino, J., Willison, H.J., Rinaldi, S., Bennett, D.L.H., Apr. 2017. Co-cultures with stem cell-derived human sensory neurons reveal regulators of peripheral myelination. Brain 140 (4), 898–913.
Dimos, J.T., et al., Aug. 2008. Induced pluripotent stem cells generated from patients with ALS can be differentiated into motor neurons. Science 321 (5893), 1218–1221.
Du, Z.-W., et al., Mar. 2015. Generation and expansion of highly pure motor neuron progenitors from human pluripotent stem cells. Nat. Commun. 6, 6626.
Faravelli, I., et al., Jul. 2014. Motor neuron derivation from human embryonic and induced pluripotent stem cells: experimental approaches and clinical perspectives. Stem Cell Res Ther 5 (4), 87.
Galbraith, J.A., Thibault, L.E., Matteson, D.R., Feb. 1993. Mechanical and electrical responses of the squid giant axon to simple elongation. J. Biomech. Eng. 115 (1), 13–22.
Goforth, P.B., Ren, J., Schwartz, B.S., Satin, L.S., May 2011. Excitatory synaptic transmission and network activity are depressed following mechanical injury in cortical neurons. J. Neurophysiol. 105 (5), 2350–2363.
Grienberger, C., Konnerth, A., Mar. 2012. Imaging calcium in neurons. Neuron 73 (5), 862–885.
Hu, B.-Y., Zhang, S.-C., 2010. Directed differentiation of neural-stem cells and subtype-specific neurons from hESCs. Methods Mol. Biol. 636, 123–137.
Hu, B.-Y., et al., Mar. 2010. Neural differentiation of human induced pluripotent stem cells follows developmental principles but with variable potency. Proc. Natl. Acad. Sci. U. S. A. 107 (9), 4335–4340.
Inman, G.J., et al., Jul. 2002. SB-431542 is a potent and specific inhibitor of transforming growth factorbeta superfamily type I activin receptor-like kinase (ALK) receptors ALK4, ALK5, and ALK7. Mol. Pharmacol. 62 (1), 65–74.
Kang, W.H., et al., Jul. 2015. Alterations in hippocampal network activity after in vitro traumatic brain injury. J. Neurotrauma 32 (13), 1011–1019.
Karumbayaram, S., et al., Apr. 2009. Directed differentiation of human-induced pluripotent stem cells generates active motor neurons. Stem Cells 27 (4), 806–811.
Kim, D.-S., Ross, P.J., Zaslavsky, K., Ellis, J., Apr. 2014. Optimizing neuronal differentiation from induced pluripotent stem cells to model ASD. Front. Cell. Neurosci. 8, 109.
Kobold, S., Guhr, A., Kurtz, A., Löser, P., May 2015. Human embryonic and induced pluripotent stem cell research trends: complementation and diversification of the field. Stem Cell Rep. 4 (5), 914–925.
Kurtoglu, E., Nakadate, H., Kikuta, K., Aomura, S., Kakuta, A., 2017. Uniaxial stretch-induced axonal injury thresholds for axonal dysfunction and disruption and strain rate effects on thresholds for mouse neuronal stem cells. JBSE 12 (1).
Li, W., et al., May 2011. Rapid induction and long-term self-renewal of primitive neural precursors from human embryonic stem cells by small molecule inhibitors. Proc. Natl. Acad. Sci. U. S. A. 108 (20), 8299–8304.
Magou, G.C., Pfister, B.J., Berlin, J.R., Oct. 2015. Effect of acute stretch injury on action potential and network activity of rat neocortical neurons in culture. Brain Res. 1624, 525–535 Supplement C.
Mann, K., Gallen, C.L., Clandinin, T.R., Aug. 2017. Whole-Brain calcium imaging reveals an intrinsic functional network in drosophila. Curr. Biol. 27 (15), 2389–2396.e4.
Marklund, N., Bakshi, A., Castelbuono, D.J., Conte, V., McIntosh, T.K., 2006. Evaluation of pharmacological treatment strategies in traumatic brain injury. Curr. Pharm. Des. 12 (13), 1645–1680.
Maury, Y., et al., Jan. 2015. Combinatorial analysis of developmental cues efficiently converts human pluripotent stem cells into multiple neuronal subtypes. Nat. Biotechnol. 33 (1), 89–96.
Mazzara, P.G., et al., Feb. 2017. Two factor-based reprogramming of rodent and human fibroblasts into schwann cells. Nat. Commun. 8, 14088.
Miller, R.G., Oct. 1987. AAEE minimonograph #28: injury to peripheral motor nerves. Muscle Nerve 10 (8), 698–710.
Muhr, J., Graziano, E., Wilson, S., Jessell, T.M., Edlund, T., Aug. 1999. Convergent inductive signals specify midbrain, hindbrain, and spinal cord identity in gastrula stage

chick embryos. Neuron 23 (4), 689–702.
Neely, M.D., et al., Jun. 2012. DMH1, a highly selective small molecule BMP inhibitor promotes neurogenesis of hiPSCs: comparison of PAX6 and SOX1 expression during neural induction. ACS Chem. Neurosci. 3 (6), 482–491.
Ogata, K., Naito, M., Feb. 1986. Blood flow of peripheral nerve effects of dissection, stretching and compression. J. Hand Surg. Br. 11 (1), 10–14.
Patani, R., et al., 2011. Retinoid-independent motor neurogenesis from human embryonic stem cells reveals a medial columnar ground state. Nat. Commun. 2, 214.
Pfister, B.J., Weihs, T.P., Betenbaugh, M., Bao, G., May 2003. An in vitro uniaxial stretch model for axonal injury. Ann. Biomed. Eng. 31 (5), 589–598.
Povlishock, J.T., Hayes, R.L., Michel, M.E., McINTOSH, T.K., Dec. 1994. Workshop on animal models of traumatic brain injury. J. Neurotrauma 11 (6), 723–732.
Prado, G.R., Ross, J.D., Deweerth, S.P., Laplaca, M.C., Dec. 2005. Mechanical trauma induces immediate changes in neuronal network activity. J. Neural Eng. 2 (4), 148–158.
Rickett, T., Connell, S., Bastijanic, J., Hegde, S., Shi, R., Oct. 2011. Functional and mechanical evaluation of nerve stretch injury. J. Med. Syst. 35 (5), 787–793.
Robinson, L.R., Jun. 2000. Traumatic injury to peripheral nerves. Muscle Nerve 23 (6), 863–873.
Rostock, C., Schrenk-Siemens, K., Pohle, J., Siemens, J., Dec. 2017. Human vs. mouse nociceptors - similarities and differences. Neuroscience 387, 13–27.
Salimi, A., Nadri, S., Ghollasi, M., Khajeh, K., Soleimani, M., Mar. 2014. Comparison of different protocols for neural differentiation of human induced pluripotent stem cells. Mol. Biol. Rep. 41 (3), 1713–1721.
Sances, S., et al., Apr. 2016. Modeling ALS with motor neurons derived from human induced pluripotent stem cells. Nat. Neurosci. 19 (4), 542–553.
Sherman, S.A., Phillips, J.K., Costa, J.T., Cho, F.S., Oungoulian, S.R., Finan, J.D., Sep. 2016. Stretch injury of human induced pluripotent stem cell derived neurons in a 96 well format. Sci. Rep. 6, 34097.
Shimojo, D., et al., Dec. 2015. Rapid, efficient, and simple motor neuron differentiation from human pluripotent stem cells. Mol. Brain 8 (1), 79.
Skotak, M., Wang, F., Chandra, N., Mar. 2012. An in vitro injury model for SH-SY5Y neuroblastoma cells: effect of strain and strain rate. J. Neurosci. Methods 205 (1), 159–168.
Sun, W., Fu, Y., Shi, Y., Cheng, J.-X., Cao, P., Shi, R., Feb. 2012. Paranodal myelin damage after acute stretch in Guinea pig spinal cord. J. Neurotrauma 29 (3), 611–619.
Sun, A.X., et al., Aug. 2016. Direct induction and functional maturation of forebrain GABAergic neurons from human pluripotent stem cells. Cell Rep. 16 (7), 1942–1953.
Surmacz, B., Fox, H., Gutteridge, A., Fish, P., Lubitz, S., Whiting, P., Sep. 2012. Directing differentiation of human embryonic stem cells toward anterior neural ectoderm using small molecules. Stem Cells 30 (9), 1875–1884.
Takahashi, K., et al., Nov. 2007. Induction of pluripotent stem cells from adult human fibroblasts by defined factors. Cell 131 (5), 861–872.
Tao, Y., Zhang, S.-C., Nov. 2016. Neural subtype specification from human pluripotent stem cells. Cell Stem Cell 19 (5), 573–586.
Topp, K.S., Boyd, B.S., Jan. 2006. Structure and biomechanics of peripheral nerves: nerve responses to physical stresses and implications for physical therapist practice. Phys. Ther. 86 (1), 92–109.
Wang, X., Gruenstein, E.I., Sep. 1997. Mechanism of synchronized ca2+ oscillations in cortical neurons. Brain Res. 767 (2), 239–249.
Xiong, Y., Mahmood, A., Chopp, M., Feb. 2013. Animal models of traumatic brain injury. Nat. Rev. Neurosci. 14 (2), 128–142.
Zeng, H., et al., Jul. 2010. Specification of region-specific neurons including forebrain glutamatergic neurons from human induced pluripotent stem cells. PLoS One 5 (7), e11853.
Zhang, P., Xia, N., Reijo Pera, R.A., Sep. 2014. Directed dopaminergic neuron differentiation from human pluripotent stem cells. J. Vis. Exp. 91, 51737.
Zhou, J., Su, P., Li, D., Tsang, S., Duan, E., Wang, F., Oct. 2010. High-effciency induction of neural conversion in human ESCs and human induced pluripotent stem cells with a single chemical inhibitor of transforming growth factor beta superfamily receptors. Stem Cells 28 (10), 1741–1750.